HHS Public Access

Author manuscript

Analyst. Author manuscript; available in PMC 2016 February 07.

Published in final edited form as:

Analyst. 2015 February 7; 140(3): 716–723. doi:10.1039/c4an01775g.

Glucose-Sensitive Nanofiber Scaffolds with Improved Sensing Design for Physiological Conditions

Mary K. Balaconis[#1], **Yi Luo**[#2], and **Heather A. Clark**[2,*]

[1]Department of Bioengineering, Northeastern University, 206 TF, 360 Huntington Avenue, Boston, MA 02115

[2]Department of Pharmaceutical Sciences Northeastern University, 206 TF, 360 Huntington Avenue, Boston, MA 02115

[#] These authors contributed equally to this work.

Abstract

Continuous physiological monitoring of electrolytes and small molecules such as glucose, creatinine, and urea is currently unavailable but achieving such a capability would be a major milestone for personalized medicine. Optode-based nanosensors are an appealing analytical platform for designing *in vivo* monitoring systems. In addition to the necessary analytical performance, such nanosensors must also be biocompatibile and remain immobile at the implantation site. Blood glucose in particular remains a difficult but high-value analyte to continuously monitor. Previously, we developed glucose-sensitive nanosensors that measure glucose by a competitive binding mechanism between glucose and a fluorescent dye to 4-carboxy-3-fluorophenyl boronic acid. To improve the sensitivity and residency time of our reported sensors, we present here a series of new derivatives of 4-carboxy-3-fluorophenyl boronic acid that we screened in macrosensor format before translating into a nanofiber format with electrospinning. The lead candidate was then implanted subdermally and its residency time was compared to spherical nanosensor analogues. The nanofiber scaffolds were markedly more stable at the implantation site whereas spherical nanosensors diffused away within three hours. Based on the enhanced sensitivity of the new boronic acids and the residency time of nanofibers, this sensor configuration is an important step towards continuous monitoring for glucose and other analytes.

INTRODUCTION

Continuously monitoring physiological analytes such as electrolytes and glucose may revolutionize disease diagnosis and management by enabling patients and physicians to accurately track an individual's analyte levels and fluctuation patterns. Implantable nanosensors offer a promising platform for physiologic monitoring because their small size makes implantation minimally-invasive, and the small suite of biocompatible polymers already FDA-approved for implant coatings and catheters provides a safe starting point for material selection. Optode-based nanosensors are robust tools for continuous and reversible

[*]Correspondence: Heather A. Clark, Ph.D, h.clark@neu.edu.

Electronic Supplementary Information (ESI) available: ^{1}H NMR data and Figure S1-3. See DOI: 10.1039/b000000x/

physiological analyte measurements, and several designs have already successfully monitored glucose, histamine, and sodium *in vivo*.[1-3] In optode-based nanosensors, reviewed extensively elsewhere[4-6], a hydrophobic plasticized polymer matrix provides support for hydrophobic analyte recognition elements and hydrophobic reporters. When the recognition element binds to its target analyte, the binding event causes a change in the local environment (e.g.; pH change, charge movement, oxygen consumption) and the reporter's optical properties change concomitantly. Nanosensors designed around optodes are essentially nanoparticles that incorporate the recognition and reporting chemistries. The components are contained within the hydrophobic nanoparticle and the resulting nanosensors' analytical properties can be tuned by changing the relative ratio of sensing components within the nanoparticle.

Previous works evaluating optode-based nanosensors for bio-analyte monitoring have used platforms such as a sliver sensor, which contained individual sensing capsules on a cellulose acetate support.[7,8] Others, such as McShane, have encapsulated sensing and reporting chemistries for glucose contained within alginate microspheres and subcutaneously injected those microspheres into rats for glucose monitoring.[9] The eventual clinical utility of any nanosensor will depend on the nanosensors' sensitivity, selectivity, biocompatibility, reversibility, response time, appropriate residency and clearance time.[10] To date, no implantable nanosensor system meets the clinical requirements for all of those factors.

Any sensor will have a recognition element and a reporting element, and personal glucometers often use the enzyme glucose oxidase and then use electrochemistry to detect the enzyme's activity in response to blood glucose from a finger prick. Alternatively, non-enzymatic recognition elements such as concanavalin A, a lectin that specifically and reversibly binds to polysaccharides via hydrogen bonds and van der Waals interaction[11], or boronic acids, which reversibly bind to diols through boronate ester formation[12,13] can detect glucose. Based on the formation of borate ester, Zhou and coworkers developed SPR[14] and fluorescence[15] based microgels to sense glucose. Borate ester formation increases through the addition of electron withdrawing groups to the boronic acid, strengthening diol binding.[16-19] Asher and coworkers used this approach by incorporating a fluoro- electron-withdrawing group onto their boronic acid derivative and were able to monitor glucose at pH 7.4 with their photonic crystal glucose sensing material.[17,20] Using carbon nanotube-based sensors, Strano and coworkers also showed that boronic acids with electron-withdrawing groups such as chloro-and cyano- groups were optimal for their sensing design.[21] Thus, we hypothesize that the sensitivity of boronic acids to glucose at physiological pH can be tuned by increasing or decreasing the electro-withdrawing ability of functional groups on a boronic acid derivative. We aim to design optode-based nanosensors that respond to physiologic glucose concentrations by synthesizing hydrophobic boronic acids with electron-withdrawing groups and fabricating nanosensors with those boronic acids. The optical reporter in this design is alizarin, which contains a diol group that can bind to boronic acids. When bound to a boronic acid, it fluoresces very strongly, but its fluorescence decreases when displaced from the boronic acid through competition with glucose. This displacement is dependent on the concentration of glucose in the surrounding solution. Of note, due to the lipophilic nature of the plasticized fiber, glucose is extracted

into the matrix upon binding to the boronic acid at the surface. It was important to explore lipophilic boronic acid derivatives to ensure that there was minimal leaching of this key component from the matrix.

A variety of nanosensors have been developed for *in vivo* glucose monitoring, but many of them have a limited residence time at the site of injection.[1] Despite their short residency time, the *in vivo* experiments showed that fluorescent glucose-responsive nanosensors are able to track changes in glucose levels for up to one hour.[1] Similar results were observed with sodium-sensitive nanosensors, and short *in vivo* lifetimes were attributed to particle migration away from and cellular uptake at the injection site.[3] Various approaches have been used to overcome these issues by immobilizing nanosensors within gels,[22] or producing high aspect-ratio sensor geometry.[23] Gel immobilization improved sensor residence time at the injection site over the course of one hour, but it did not provide a long-term solution to sensor migration because nanosensors are small enough to diffuse out of the gels.[22] Our group previously demonstrated that encapsulating nanosensors into worm-like geometries with chemical vapor deposition prevented the signal loss associated with diffusion away from the injection site,[23] though the chemical vapor deposition fabrication methods used in that study have low batch yields. Electrospinning is a high-yield process that can fabricate continuous polymer nanofibers of optode material. With nanofiber geometries, implanted nanosensors may achieve a residency time in conjunction with a high throughput and scalable production technique while retaining advantages of nano-scale sensors.[24] Although other groups have utilized electrospinning to fabricate sensors for detecting silver,[25] mercury,[26] nitroaromatics,[27] and glucose,[28,29] none have shown that their sensor design functions *in vivo*.

In this work, to improve the stability of our previously presented[1] glucose-sensitive nanosensors, we fabricated nanofiber scaffolds from plasticized polycaprolactone and incorporated the best of the boronic acid derivatives with alizarin to show that this sensor platform exhibits extended *in vivo* sensor residency time.

In addition, we functionalized 4-carboxy-3-fluorophenyl boronic acid with hydrophobic alkyl side chains of varying lengths to increase the nanosensors' stability to leaching and sensitivity to glucose, as compared to previous formulations.[1]

MATERIALS AND METHODS

Materials

Carboxylatedpoly(vinyl chloride) (>97% GC) (PVCCOOH), *bis*-(2-ethylhexyl)sebacate (DOS), polycaprolactone (M_n 70,000-90,000) (PCL), tridodecylmethylammonium chloride (TDMAC), alizarin, 4-carboxy-3-fluorophenylboronic acid (**1**), 3-fluoro-4-methoxycarbonylphenylboronic acid (**2a**), *D*-(+)-glucose, tetrahydrofuran (≥ 99.9%) (THF), dicyclohexylcarbodiimide solution (60% w/v in xylene) (DCC), *N*-hydroxysuccinimide (NHS), aniline(≥ 99.5%), 1-propanol (anhydrous, 99.7%), 1-butanol (HPLC, 99.7%), 1-hexanol (98%), cyclohexanol(99%),sodium sulfate (anhydrous,≥ 99.9%), sodium chloride, ethyl acetate (anhydrous, 99.8%), hexane (anhydrous, 99.5%), *N*, *N*'-dimethylformamide (DMF) and *N*, *N*'-dimethylaminopyridine (DMAP) were purchased from Sigma Aldrich (St

Louis, MO, USA). Octylboronic acid (>97%) and Citroflex A-6 were acquired from Synthonix (Wake Forest, NC, USA) and Vertellus (Indianapolis, IN, USA), respectively. Phosphate Buffered Saline (PBS) (1x, pH = 7.4) was purchased as a solution from Invitrogen (Carlsbad, CA, USA). Hydrochloric acid (1.0 N) and sodium bicarbonate were purchased from Fisher Scientific (Fair Lawn, NJ, USA). 1,2-distearoyl-*sn*glycero-3-phosphoethanolamine-N-[methoxy(polyethylene glycol)-550] (ammonium salt) (DSPE-mPEG550) was purchased from Avanti Polar Lipids, Inc. SKH1-E mice were acquired from Charles River Laboratories International Inc. (Wilmington, MA).

Boronic Acid Synthesis

To control the response, we systematically functionalized **BA1** with alkyl chains of various lengths (Figure 1). The synthesis protocol has been previously developed by Steglich and coworkers. [30] Specifically, 200 mg of **BA1** (1.09 mmol, 1 Eq.) was mixed with 40 mg DMAP (0.33 mmol, 0.3 Eq.) and alcohol **2** (3.27 mmol, 3 Eq.) in 4 mL DMF. DCC solution in xylene (60% w/v) (1.09 mmol, 1 Eq.) (220 μL) was added dropwise to the reaction mixture at 0° C, which was then warmed to room temperature and stirred overnight. The urea precipitate was removed by centrifugation and then the supernatant was extracted with 20 mL ethyl acetate and 0.5 M HCl aqueous solution. This process was repeated three times. The product was washed with saturated $NaHCO_3$ aqueous solution and then brine (saturated sodium chloride solution). The organic phase was dried over Na_2SO_4 and further purified by flash column chromatography. The product was characterized by ^1H NMR recorded on a Varian Inova 500 MHz NMR spectrometer. ^1H NMR data is available in the supplementary information.

Optode Composition

Macrosensors, nanofiber scaffolds, and nanoparticle-based sensors were formed from optode cocktails containing all sensing components. Macrosensors were made from the following components: 30 mg PCL, 60 μL Citroflex A6, 83.3 μmol of a boronic acid (BA) derivative (**BA2b** – **BA2c**), 2.0 mg (3.49 μmol) TDMAC, and 1.0 mg (4.16 μmol) alizarin. These materials were placed into a glass vial and then dissolved in 500 μl THF. The boronic acids incorporated into these formulations were **BA1**, and **BA2a-c**. For production of electrospun scaffolds, the general optode cocktail was made with a solution of 12% (weight/volume) of PCL in Citroflex A-6 and THF. Of this weight percentage, 10% was Citroflex A-6. Specifically, the optode formulation was: 216 mg PCL, 24.0 μL Citroflex A-6, 2.0 mg (3.49 μmol) TDMAC, 1.0 mg (4.16 μmol) alizarin, and 83.3 μmol boronic acid in 2 ml THF. Three boronic acids, **2a**, **2b** and **2c**, were tested in electrospun scaffolds. Nanoparticle-based sensors were fabricated with an optode formulation previously described and include: 30 mg high molecular weight PVC-COOH, 60 μl DOS, 3.0 mg octylboronic acid, 4.0 mg TDMAC, and 1.0 mg alizarin.[1] These materials were transferred into a glass vial and then dissolved in 500 μl THF.

Response of Macrosensors to Glucose

Prior to miniaturization to the nanoscale, each new **BA** was assessed as a glucose-sensitive macrosensor. The method for testing macrosensor responses has been described previously.[1]

Briefly, macrosensors are formed by pipetting 2 μL of optode onto glass discs adhered to the bottom of an optical bottom 96-well plate. The optodes were then allowed to dry at least 15 minutes forming thin film macrosensors. A Spectramax Gemini EM microplate fluorometer (Molecular Devices, Sunnyvale, CA, USA) acquired fluorescence data (ex/em: 460/570 nm). After forming macrosensors, each macrosensor was hydrated in 200 μL PBS (pH=7.4) for 45 minutes. This process was repeated 4 times until the fluorescence intensity stabilized. After the macrosensors were hydrated, the PBS solution was removed from all wells and 200 μl of 0.1 M glucose in PBS was pipetted into half of the wells to determine macrosensor response to glucose. The remaining wells acted as controls and contained fresh, glucose-free PBS. Changes in fluorescence response were monitored for 60 minutes at a sampling rate of 5 minutes. The fluorescence intensity of each sensor was normalized to time zero and then the mean was taken for both the experimental and control groups. The average of the experimental group was subtracted from the control group and multiplied by 100 to obtain a percent change. The error of percent change was calculated using error propagation.

Fabrication of Fibrous Scaffolds

Electrospinning was performed on a Nanospinner NE 200 (Inovenso, Istanbul, Turkey) equipped with a syringe pump. The optode solution was spun at a distance of 10 cm from the collector with a rate of 3 ml/hr and at an applied voltage of 15 kV. The fibers were spun onto either aluminum foil or silanized glass discs attached to aluminum foil for imaging and testing scaffold response, respectively.

Nanofiber Scaffold Responses to Glucose

To determine scaffold response to glucose, scaffolds spun onto glass discs were removed from the aluminum foil using a 6 mm biopsy punch (Miltex, Inc., Plainsboro, NJ, USA) and placed in a 96-well optical bottom well plate. PBS (200 μL) was added to each well and the sensors were hydrated in PBS overnight to stabilize the fluorescence intensity. All fluorescence measurements (ex/em: 460/570 nm) were acquired using a SpectraMax Gemini EM plate reader. After hydration, the PBS was replaced with 200 μL of fresh PBS (pH 7.4) as a control or 0.1 M glucose in PBS (pH 7.4). The fluorescent responses were measured for 60 minutes at 5-minute intervals. Fluorescence measurements were normalized to the first time point and averaged for each experimental group. The average response of the experimental group was subtracted from the control group and then plotted over time. Error was determined using error propagation.

Fluorescence Imaging

Images of scaffolds were acquired on a Zeiss Confocal Microscope (Thornwood, NY) using a 488 nm laser and 10x air objective (PlanApo, NA = 0.17).The laser intensity was set to 1% (10 mW full power)

SEM Acquisition

Images of scaffolds were acquired on a Hitachi S4800 with a 5 kV accelerating voltage. Samples were not sputter coated. Fiber diameters were measured using Quartz PCI (Quartz Imaging Corp.) software. Magnification was 10X, and numerical aperture was 0.45 in.

Fabrication of Nanoparticle-based Sensors

The fabrication of nanoparticle-based sensors is described previously. [1] Briefly, the optode was dried overnight on a glass plate, and then transferred into a scintillation vial. Then 5 ml of PBS (pH=7.4) and 5 mg of DSPE-mPEG(550) in 500 μL of chloroform was added. The mixture was sonicated for 3 minutes at 40% amplitude using a Branson digital sonifier (Danbury, CT).The nanosensor solution was pipetted out from vial leaving residual optode.

In Vivo Studies

Animal procedures were approved by Northeastern University's Institutional Animal Care and Use Committee. To determine whether nanofiber scaffolds minimized sensor diffusion *in vivo*, glucose nanosensors and scaffolds were prepared as above. Scaffolds were cut into circular pieces using a 6 mm diameter biopsy punch and sterilized by soaking in 70% ethanol and then sterile PBS (pH=7.4). SKH1-E mice were anesthetized and then injected with 20 μL of either nanosensors or scaffolds along their backs. To determine the injection volume, the amount of sensor material in a 6 mm diameter scaffold was estimated and then approximated to the same amount of material in the nanosensor formulation. Nanosensors were injected with 31G insulin syringes (BD Biosciences, Franklin Lakes, NJ). Scaffolds were injected using an indwelling needle assembly.[31] The assembly consisted of a 20 G outer needle and a 25 G inner needle with a blunted tip that acted as the plunger. 3M Vetbond ™ tissue adhesive (3M Animal Care Products, St. Paul, MN) was then applied to the injection site. Imaging was performed on an IVIS Lumina II (Perkin Elmer) small animal imager in fluorescence mode with a 465/30 excitation filter and 580/20 emission filter. Mice were imaged every 5 minutes for 1 hour and then at 3 hours post-injection. Fluorescence measurements were analyzed by selecting a region of interest around each injection spot to obtain the total radiant efficiency of the area. The background-subtracted total radiant efficiency from each region of interest containing either scaffolds or nanosensors was measured at each time point and then normalized to the total radiant efficiency at time 0. The normalized values were then averaged across three mice for both the scaffolds and nanosensors. To account for sensor degradation over time, scaffolds and nanosensors were prepared as above and placed into a 96-well plate with a total volume of 200 μL of either PBS or PBS and nanosensors. Their total radiant efficiency was tracked using the same imaging parameters and data analysis as the *in vitro* studies.

RESULTS AND DISCUSSION

Boronic Acid (BA) Selection

The clinical utility of glucose-responsive nanosensors depends on their ability to exhibit proper dynamic range and sensitivity.[7] In the sensors presented here, the boronic acid sensing moiety governs the sensor response to glucose. The sensors respond to glucose by a competitive binding interaction between boronic acids and diols on either alizarin or glucose. In the absence of glucose, the boronic acid binds to the diol on alizarin, statically quenching its fluorescence. As local glucose concentrations increase, those molecules displace the alizarin, allowing it to fluoresce.

We derived phenylboronic acids containing fluoro- and carboxyl- groups that withdraw electrons in order to improve sensor response compared to octylboronic acid, which was used previously.[1] Comparing boronic acid used in this paper to octylboronic acid, the fluorescence was enhanced by 10%. In addition to acting as an electron-withdrawing group, carboxyls provide a site for the alkyl chain additions performed herein and other chemical modifications. The initial screen for glucose-responsiveness showed that macrosensors with 4-carboxy-3-fluorophenyl boronic acid (**BA1)** increased in fluorescence by 13% from baseline in response to 100 mM glucose (Figure 2). This compound's reactivity derives from having both fluoro- and carboxyl groups withdrawing electrons from the boronic acid group, however, this increases the compound's polarity. Consequently, **BA1** readily leached from the hydrophobic sensor platform over time (Figure S1), which led to signal degradation and loss of sensitivity to glucose. We then produced a new set of boronic acid molecules with varying polarities by systematically converting the carboxyl group into esters with various alkyl chain lengths to find responsive and stable sensors.

Adding a methyl ester to **BA1** produced **BA2a**, which leached out of the macrosensors significantly less than **BA1**, and longer alkyl chains (**BA2b** &**BA2c**) produced no significant reduction in leaching compared to the methyl ester (Figure S1). Improvement in stability when replacing the carboxylate ligand to an ester suggests that the leaching of boronic acid may play an important role. Increasing the alkyl length decreased the resulting boronic acid's reactivity; the magnitude of macrosensor responses to glucose when formulated with **BA2a**, **BA2b**, and **BA2c** were all less compared to macrosensors made with **BA1**. Macrosensors with **BA2a** were still relatively sensitive at physiological pH, exhibiting a 10% increase in fluorescence in response to 100 mM glucose. By contrast, macrosensors made with **BA2b** and **BA2c** only increased by 3% and less than 1%, respectively (Figure 2).

The nanosensors' competitive binding mechanism depends on the boronic acid diffusing within the hydrophobic matrix and interacting with glucose molecules at the sensor-environment interface. The result that longer alkyl chains reduced the magnitude of sensor responses suggests that long alkyl chains inhibited boronic acid diffusion within the polymer matrix. While leaching is much less problematic for those derivatives such as **BA2c**, the increased hydrophobicity may impart too high of an affinity to polymer matrix, causing sluggish diffusion and small sensor responses.

Analysis of the calibration curve displays a 10 fold change between 30 mM and 100 mM glucose (Figure S2). To examine the selectivity of the formulation as compared to other sugars, fructose was tested *in vitro*. The signal intensity of the 1 mM fructose solution was about half that of the 100 mM glucose after 1 h of incubation (Figure S3). We chose to compare 1 mM fructose because it is present in the body at a concentration of about 8 μM[32], so we tested it at 100 fold excess, as we did with the glucose. Considering the difference in the comparative concentrations of these sugars in the body, the interference is at an acceptable, if not optimal, level. We anticipate that other monosaccharides in interstitial fluid may also bind to boronic acid, but these would be present at very low physiological concentrations.

Our previous glucose-sensitive nanosensors included octylboronic acid, a hydrophobic aliphatic derivative, as the sensing moiety,[1,33] because it was stable in the hydrophobic nanosensor core. [16,34] Despite their stability, nanosensors with octylboronic acid were not sufficiently sensitive to glucose. From studies on optodes, we discovered that 4-carboxyl-3-fluoroboronic acid **1** and its derivatives are more sensitive to glucose due to their fluoro- and carboxyl groups. With the results showing that **BA2a** leaches significantly less than **BA1** and is much more responsive to glucose than **BA2b** and **BA2c**, **BA2a** was selected as the lead candidate for nano-scale sensor fabrication.

Glucose-Sensitive Nanofibers

In addition to improvements in nanosensor sensitivity, nanosensor systems need new design strategies for increasing residency time at the implantation site, ideally with minimally-invasive delivery methods. Glucose nanosensors with **BA2a** were electrospun to produce nanosensors with nanofiber architectures, requiring a plasticizer content of 10%.

For comparison, spherical nanosensors were also made using the fabrication method described in the Materials and Methods section. Electrospinning optodes with 70 – 90 kDa PCL successfully produced continuous polymer nanofibers, as confirmed with SEM images for high resolution fiber measurements and with confocal images to show homogenous fluorescence from the alizarin within the fibers (Figure 3). Measurements from the SEM images indicate that fiber diameters were 374 ± 142 nm and were continuous without beading or wetting. Optode-based sensors are typically highly plasticized to aid the mobility of sensor components and analytes within the sensor.[35] Nanofibers that were electrospun with PCL and 30% or 60% plasticizer increased the glucose-sensitivity by 6%, as expected. However, even the 30% plasticized scaffolds showed signs of electrospinning instability with discontinuous fibers and areas of pools of plasticizer (data not shown). Therefore in order to maintain the nanofibrous structure, we used 10% plasticizer content at the trade-off of sensor response.

Glucose-sensitive nanofibers with **BA2a**, **2b** and **2c** responded 2% less, 2% more and 1% less than their macrosensor counterparts, respectively. Boronic acids with longer alkyl chains decreased the sensitivity to glucose. To test the electrospun nanosensor response times, fluorescence intensity was monitored over one hour after placing scaffolds in 100 mM glucose in PBS. Sensors containing **BA2b** reached 95% of their maximum response within 12 minutes, but sensors containing **BA2a** did not level off within an hour (Figure 4). The slow response times are likely due to the low plasticizer content as well as the static flow conditions for the experimental configuration. Low plasticizer content would restrict components from diffusing to the sensor-environment interface. An experiment conducted in a flow cell would have enhanced the rate of solution diffusion throughout the porous scaffold and decreased the response time. Despite these slow response times, it is important to note that physiologic glucose levels change over the course of tens of minutes,[36] meaning that the **BA2b** formulation in nanofiber form responds sufficiently fast to capture these changes.[7] Higher molecular weight PCL or other polymers can support higher plasticizer percentage.

For example, electrospun nanofibers fabricated with ethyl cellulose were able to support up to40% plasticizer.[23] Such strategies offer additional ways to improve the sensitivity and response times of future nanosensor designs.

Non-specific protein binding is prevented by this structure since only small molecules or ions can be extracted into the organic polymers.

In Vivo Lifetime Studies

In previous *in vivo* studies, nanoparticle-based sensors diffused away from the implantation site within one hour. To show that nanofiber nanosensors improve residency times at the implantation site, either spherical nanosensors or nanofiber nanosensors were implanted subdermally (Figure 5) and their signal loss was directly compared to their *in vitro* signal loss. Similar to previous experiments, the spherical nanosensors lost radiant efficiency at the injection site significantly greater than the signal loss observed *in vitro*. *In vitro* signal loss is attributed to boronic acid leaching from the hydrophobic core, and the difference between *in vivo* and *in vitro* signal loss is attributed to nanosensor diffusion away from the implantation site. By contrast, nanofiber scaffolds exhibited very closely matched signal loss between the *in vivo* and *in vitro* experiments after one hour, and they were nearly equal after three hours (Figure 6). The spherical nanosensors experienced a ~30% difference in total radiant efficiency loss when compared to the *in vitro* control, whereas the decay constants for nanofiber scaffolds differed only by 6%.

Several factors accelerated the signal loss for spherical nanosensors *in vivo* compared to *in vitro*, most notably sensor diffusion, cellular uptake, and the potential for facilitated transport of components (either alizarin or boronic acid) out of the nanosensors due to amphiphilic serum components in the *in vivo* environment.

Since the *in vivo* lifetime of the nanofiber scaffold compared to the nanoparticles was increased almost to the levels observed with the nanofibers *in vitro*, we could conclude that the new sensor geometry maintained sensor residency at the injection site and would allow for longer monitoring times.

CONCLUSION

In this study, we developed optode-based glucose nanosensors that were more sensitive to glucose and more stable at the site of *in vivo* implantation.[20] The initial macrosensor screen showed that electron-withdrawing groups on **BA1** and its derivatives facilitated a response to glucose under physiological conditions, which is a major improvement over previous hydrophobic boronic acid derivatives. Using the most responsive hydrophobic boronic acid derivative, **BA2a**, nanosensors were electrospun into nanofibers and the nanofiber format was significantly more stable *in vivo* than spherical nanosensors. Future work will focus on further increasing sensitivity and stability by red-shifting the reporters and adding a reference signal for quantitative measurements.

Supplementary Material

Refer to Web version on PubMed Central for supplementary material.

ACKNOWLEDGMENTS

This work was supported by the National Institute of Health under award number 5RO1GM084366 and Northeastern University's internal funding Tier 1 support. Additionally, we thank Chris Skipwith for his help in obtaining SEM images, Roger Kautz for his help in obtaining NMR spectra, and Ganesh Thakur for his help with flash column chromatography.

Notes and references

1. Billingsley K, Balaconis MK, Dubach JM, Zhang N, Lim E, Francis KP, Clark HA. Anal Chem. 2010; 82:3707. [PubMed: 20355725]
2. Cash KJ, Clark HA. Anal Chem. 2013; 85:6312. [PubMed: 23767828]
3. Dubach JM, Lim E, Zhang N, Francis KP, Clark H. Integrative Biology. 2011; 3:142. [PubMed: 21088796]
4. Bakker E, Buhlmann P, Pretsch E. Chem Rev. 1997; 97:3083. [PubMed: 11851486]
5. Bakker E, Simon W. Analytical Chemistry. 1992; 64:1805.
6. Buhlmann P, Pretsch E, Bakker E. Chem Rev. 1998; 98:1593. [PubMed: 11848943]
7. Tohda K, Gratzl M. Chemphyschem. 2003; 4:155. [PubMed: 12619414]
8. Tohda K, Gratzl M. Analytical Sciences. 2006; 22:383. [PubMed: 16733308]
9. Srivastava R, Jayant RD, Chaudhary A, Mcshane MJ. Journal of Diabetes Science and Technology. 2011; 5:76. [PubMed: 21303628]
10. Ruckh TT, Clark HA. Implantable nanosensors: toward continuous physiologic monitoring. Anal Chem. [Online Early Access]. Published Online: 2014.
11. Loris R, Hamelryck T, Bouckaert J, Wyns L. Biochem. & Biophys. Acta. 1998; 1383:9. [PubMed: 9546043]
12. Springsteen G, Wang BH. Tetrahedron. 2002; 58:5291.
13. Yan J, Springsteen G, Deeter S, Wang BH. Tetrahedron. 2004; 60:11205.
14. Wu W, Shen J, Li Y, Zhu H, Barnerjee P, Zhou S. Biomaterials. 2012; 33:7115. [PubMed: 22800540]
15. Li Y, Zhou S. Chem. Commun. 2013; 49:5553.
16. Mulla HR, Agard NJ, Basu A. Bioorganic & Medicinal Chemistry Letters. 2004; 14:25. [PubMed: 14684290]
17. Das S, Alexeev VL, Sharma AC, Geib SJ, Asher SA. Tetrahedron Letters. 2003; 44:7719.
18. Singhal RP, Ramamurthy B, Govindraj N, Sarwar Y. Journal of Chromatography. 1991; 543:17.
19. Liu XC, Scouten WH. Journal of Chromatography A. 1994; 687:61.
20. Alexeev VL, Sharma AC, Goponenko AV, Das S, Lednev IK, Wilcox CS, Finegold DN, Asher SA. Anal Chem. 2003; 75:2316. [PubMed: 12918972]
21. Yum K, Ahn JH, McNicholas TP, Barone PW, Mu B, Kim JH, Jain RM, Strano MS. ACS Nano. 2012; 6:819. [PubMed: 22133474]
22. Balaconis MK, Clark HA. J Diabetes Sci Technol. 2013; 7:53. [PubMed: 23439160]
23. Ozaydin-Ince G, Dubach JM, Gleason KK, Clark HA. Proc. Natl. Acad. Sci. U. S. A. 2011
24. Cash KJ, Clark HA. Trends in Molecular Medicine. 2010; 16:584. [PubMed: 20869318]
25. Kacmaz S, Ertekin K, Suslu A, Ozdemir M, Ergun Y, Celik E, Cocen U. Sensors and Actuators B-Chemical. 2011; 153:205.
26. Kacmaz S, Ertekin K, Suslu A, Ergun Y, Celik E, Cocen U. Materials Chemistry and Physics. 2012; 133:547.
27. Yang YF, Wang HM, Su K, Long YY, Peng Z, Li N, Liu F. Journal of Materials Chemistry. 2011; 21:11895.

28. Manesh KM, Santhosh P, Gopalan A, Lee K-P. Analytical Biochemistry. 2007; 360:189. [PubMed: 17123457]
29. Zhou CS, Shi YL, Ding XD, Li M, Luo JJ, Lu ZY, Xiao D. Anal Chem. 2013; 85:1171. [PubMed: 23215003]
30. Neises B, Steglich W. Angewandte Chemie International Edition in English. 1978; 17:522.
31. Heo YJ, Shibata H, Okitsu T, Kawanishi T, Takeuchi S. Proceedings of the National Academy of Sciences of the United States of America. 2011; 108:13399. [PubMed: 21808049]
32. Kawasaki T, Akanuma H, Yamanouchi T. Diabetes Care. 2002; 25:353. [PubMed: 11815509]
33. Balaconis MK, Billingsley K, Dubach MJ, Cash KJ, Clark HA. J Diabetes Sci Technol. 2011; 5:68. [PubMed: 21303627]
34. Alexeev VL, Das S, Finegold DN, Asher SA. Clin. Chem. 2004; 50:2353. [PubMed: 15459093]
35. Bakker E, Buhlmann P, Pretsch E. Chemical Reviews. 1997; 97:3083. [PubMed: 11851486]
36. Boyne MS, Silver DM, Kaplan J, Saudek CD. Diabetes. 2003; 52:2790. [PubMed: 14578298]

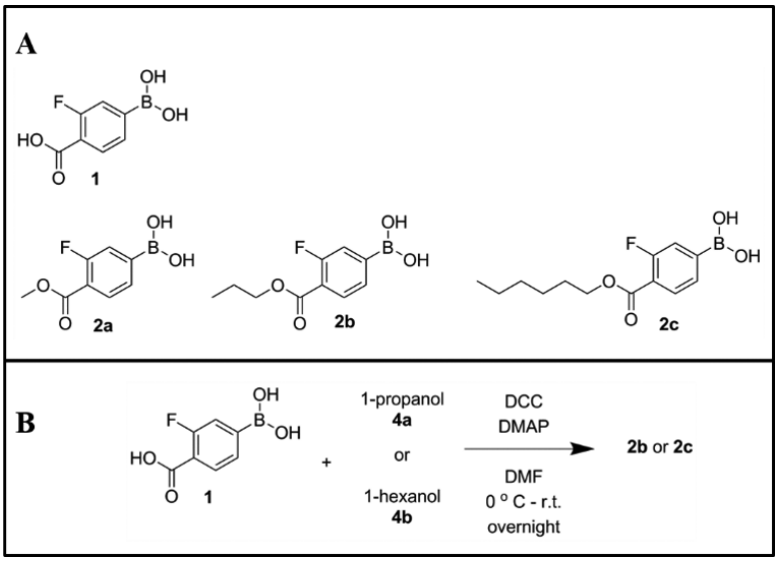

Figure 1. Boronic acids incorporated into glucose-sensitive sensors

(A) Structures and (B) synthesis of boronic acids with different alkyl chain lengths and ring structures.

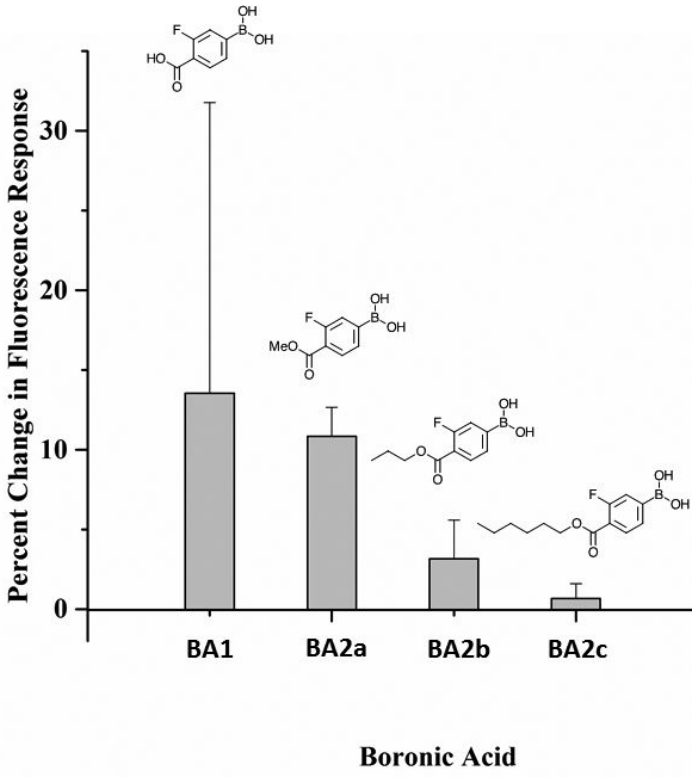

Figure 2. Response of glucose-sensitive macrosensors containing functionalized boronic acids with increasing length of alkyl chains

The macrosensors contain **Boronic Acids 1** ($n_{control}$ = 7, $n_{glucose}$ = 8), **2a** ($n_{control}$ = 7, $n_{glucose}$ = 7), **2b** ($n_{control}$ = 7, $n_{glucose}$ = 7), or **2c** ($n_{control}$ = 8, $n_{glucose}$ = 8). Macrosensors were exposed to either PBS as a control or 100 mM glucose in PBS for 60 minutes. The percent change in fluorescence response was calculated as the average normalized difference between the control and glucose groups. Error bars were calculated using error propagation.

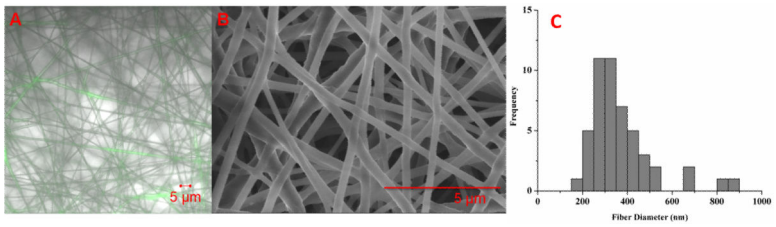

Figure 3. Electrospun glucose-sensitive scaffolds

(A) Confocal image, (B) SEM image and (C) size distribution of glucose-sensitive nanofibers. The average fiber diameter was 374 ± 142 nm (n=49). The width of histogram columns represents 50 nm.

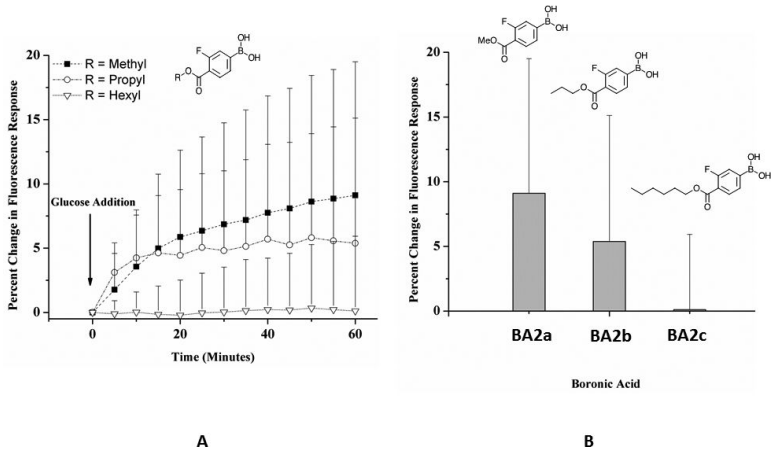

Figure 4. Response of glucose-sensitive nanofibers containing different functionalized boronic acids

Glucose-sensitive nanofibers contained fluorinated boronic acid derivatives **2a** ($n_{control}$ = 6, $n_{glucose}$ = 8), **2b** ($n_{control}$ = 5, $n_{glucose}$ = 7), and **2c** ($n_{control}$ = 7, $n_{glucose}$ = 8). (**A**) Nanofibers were exposed to either PBS as a control or 100 mM glucose in PBS for 60 minutes. Methyl and propyl borate ester sensors display a change in fluorescence reported as a percent change from baseline. (**B**) Increasing alkyl chain lengths on fluorinated boronic acid derivatives affected the response of glucose-sensitive nanofibers. The percent change in fluorescence response was calculated as the average normalized difference between the control and glucose groups. Error bars were calculated using error propagation.

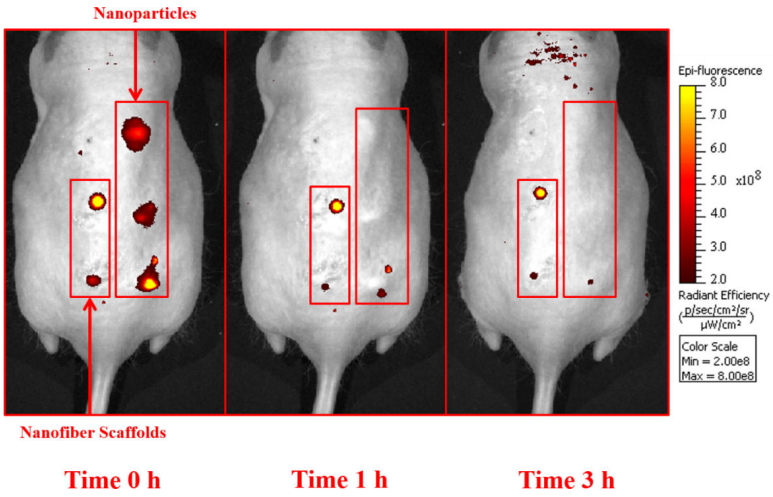

Figure 5. ***In vivo*** **comparison of glucose-sensitive nanoparticles and nanofiber scaffolds**

Mice were injected with glucose-sensitive nanoparticles and nanofiber scaffolds along their backs and then imaged with a fluorescent small animal imager for one hour and then at 3 hours post-injection. Shown here are the fluorescent images from one mouse over this time frame.

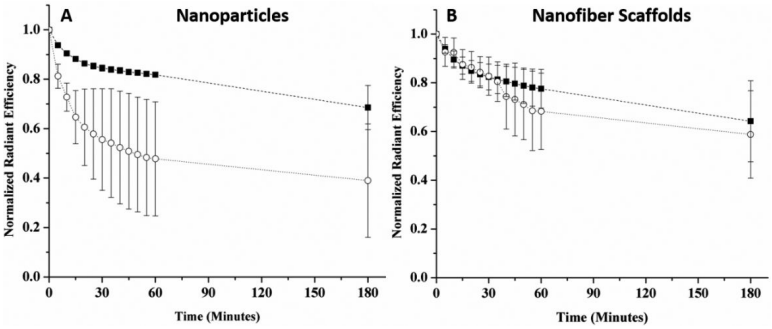

Figure 6. Fluorescence measurements of glucose-sensitive nanoparticles and nanofiber scaffolds over time *in vivo*

The average normalized total radiant efficiency of glucose-sensitive (A) nanoparticles and (B) nanofiber scaffolds both *in vivo* (○) and *in vitro* control (■) were plotted over time. The normalized *in vivo* average for nanoparticles and nanofiber scaffolds was calculated across 3 different mice with $n_{nanoparticles}$= 8 and $n_{nanofiber\ scaffolds}$= 6 injection spots. Similarly, the normalized *in vitro* average was calculated from $n_{nanoparticles}$= 8 and $n_{nanofiber\ scaffolds}$= 7. Error bars represent standard deviations.